Notes

Structural Characterization of Isomeric Dimers from the Oxidative Oligomerization of Catechol with a Biomimetic Catalyst

Daniela Šmejkalová,[†] Pellegrino Conte,[‡] and Alessandro Piccolo*,[†]

Dipartimento di Scienze del Suolo, della Pianta e dell'Ambiente, Università di Napoli Federico II, Via Università 100, 80055 Portici, Italy, and Dipartimento di Ingegneria e Tecnologie Agro-Forestali, Università di Palermo, Viale delle Scienze 13, 90128 Palermo, Italy

Received June 21, 2006
Revised Manuscript Received October 28, 2006

Introduction

Naturally occurring phenolic compounds have attracted much attention as molecular models in studies of humification processes undergone by the organic matter in soil.[1−3] Phenolic substrates involved in humus formation derive from the decomposition of plant residues or are synthesized by microorganisms from glucose and other carbohydrates.[4] In the reaction models, phenol monomers are usually subjected to oxidative coupling reactions that are generally supposed to be involved in the formation of humic-like substances.[5] The coupling reactions can be mediated by various oxidoreductase enzymes as well as by inorganic catalysts present in the terrestrial environment. Both of these catalysts are thought to mediate the oxidative coupling of humic matter by means of a radical mechanism.[4−6]

Among the humic phenols, catechol (1,2−dihydroxybenzene) is considered to be an excellent model for studying oxidative coupling since it is the simplest molecule containing the very reactive *ortho*-diphenol group, which is quickly oxidized to the corresponding semiquinone or quinone by O_2 present in the environment.[3] In soils, catechol is a constituent of humic matter and plant-derived polyphenol and acts as an intermediate in the biodegradative pathways of substituted benzenes such as aminophenol, aniline, phenol, benzoate, or even toxic aromatic compounds.[7−9]

The model catechol substrate has been subjected to polymerization reactions in the presence of mineral catalysts, such as silica,[10] alumina,[11] birnessite,[5] or silver colloid surfaces,[3] and in the presence of oxidoreductases, such as laccase,[12,13] peroxidase,[4,14] or tyrosinase.[15] Notwithstanding all of these studies, only few of them suggested the nature of the coupling products, and none gave direct evidence of the exact bonding position in the coupled products. This knowledge is fundamental not only for elucidation of the humification process but also for the possible application of similarly catalyzed oxidative coupling reactions to remove phenolic compounds from wastewaters.[16] Moreover, polyphenols synthesized by peroxidase-like reactions are of high interest also in the area of electronic and photonic devices,[9] since they possess unique electrical and optical properties due to their conjugated backbone.[17]

We showed earlier[18] the formation of catechol di-, tri- and tetramers within an oxidative polymerization catalyzed by synthetic water-soluble iron−porphyrin as an efficient alternative to bio-labile natural peroxidase. We have also demonstrated the occurrence of both C−C and C−O−C coupling mechanisms. However, since the coupling products were determined by mass spectroscopy, the exact bonding position could not have been precisely ascertained for the C−C bonded isomeric dimers that are the dominant products of catechol oligomerization. Therefore, the aim of this work was to isolate the catechol isomeric dimers obtained by oxidative coupling under the catalysis of a synthetic iron−porphyrin and determine their molecular structures by NMR spectroscopy.

Experimental Section

Biomimetic Iron−Porphyrin. Information on the synthesis, structure, and characterization of the water-soluble iron(III) meso-tetra-(2,6−dichloro-3-sulfonatophenyl)-porphyrinate [Fe(TDCPPS)Cl] used here as biomimetic catalyst is reported elsewhere.[19]

Catechol. 1,2-Dihydroxybenzene, or catechol, was purchased from Sigma-Aldrich (Germany), with a purity ranging between 97% and 99%, and was used without further purification.

Oxidative Polymerization. A 400 mg L^{-1} reaction solution of catechol was prepared by dissolving 40 mg of catechol in 3 mL of methanol, adding 70 mL of MilliQ grade water, 2.4 μmol of [Fe(TDCPPS)Cl] (22 mL of a 1.09×10^{-4} M solution), and 2.0 μL of toluene (Sigma-Aldrich, Germany; 97% purity) as a bacteriostatic agent, and reaching 100 mL with MilliQ water. After the solution was mixed thoroughly, 470 μL of a 0.017 M solution of H_2O_2 (Ashland Chemical, Italy) was added to reach a final concentration of 0.08 mM in hydrogen peroxide. After an optimum reaction time (i.e., the time when reaction products reached a maximum concentration),[20] the reaction solution was concentrated on a solid-phase extraction (SPE) column and then fractionated by high-performance liquid chromatography (HPLC).

Solid-Phase Extraction. Reaction products were extracted using a C_{18} cartridge (column dimensions, 100 mm × 4.6 mm; volume, 5 mL; Varian, USA) that was first soaked for 1 min in methanol, conditioned with 5 mL of methanol, and then equilibrated with 5 mL of water at a flow rate of 3−5 mL min^{-1}. The reaction sample (100 mL) was loaded on the column at a flow rate of 1 mL min^{-1}. After the preconcentration step, the cartridge was rinsed with 2 × 5 mL of water at a flow rate of 1−2 mL min^{-1} to remove matrix impurities. Afterward, the cartridge was dried under full vacuum for 2 min. Then, the target compounds were eluted with 1 mL of methanol at a flow rate of 1 mL min^{-1}. The extract was diluted with water to an approximate volume of 8 mL and fractionated by reverse-phase HPLC.

HPLC Fractionation. A Perkin-Elmer LC 200 pump equipped with a 1000 μL sample loop on a 7125 Rheodyne rotary injector was used for fractionation through a semipreparative C_{18} **(2)**

* Author to whom correspondence should be addressed. Phone: +39-081-2539160. E-mail: alpiccol@unina.it.
[†] Università di Napoli Federico II.
[‡] Università di Palermo.

10.1021/bm060598o CCC: $37.00
Published on Web 12/24/2006

Scheme 1. Resonance Structures 1−4 of Intermediate Radicals Generated during Iron−Porphyrin-Catalyzed Oxidation of Catechol

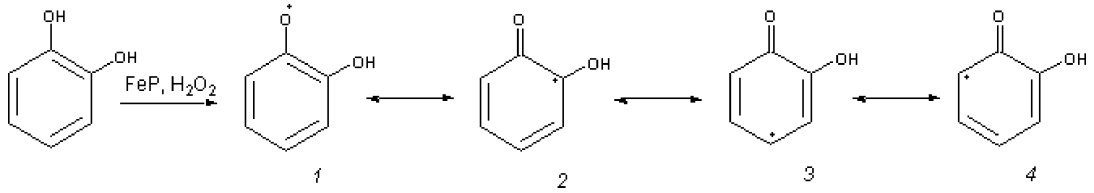

Scheme 2. Suggested Coupling Reactions between Some of the Catechoyl Radicals Leading to the Formation of C−C Coupled Dimers

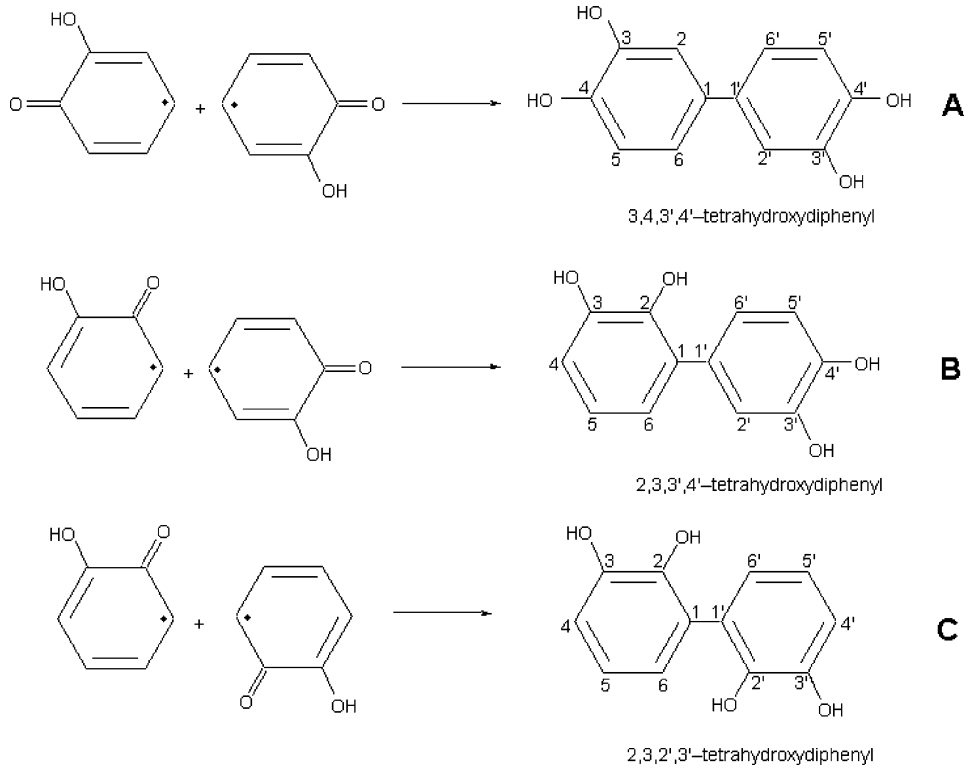

Luna column (250 mm × 10.0 mm, 10 μm; Phenomenex) held at a constant temperature of 30 °C. A Perkin-Elmer LS-3B fluorescence spectrometer, set at 278/360 nm (excitation/emission), was used to detect the reaction products.

The chromatographic eluent consisted of a binary phase made of acetonitrile (A) and a 0.75% trifluoroacetic acid solution (B) that was pumped at 1.5 mL min^{-1} with the following gradient mode: A was held for 7 min at 2%, increased to 15% over 35 min, increased to 50% over 27 min, and finally held at 50% for 5 min.

Reaction products were manually collected from (A) 56.5−58.0, (B) 63.2−63.7, and (C) 67.5−68.2 min repeatedly for eight chromatographic runs into 10 mL Pyrex test tubes and cumulatively freeze-dried. The three collected fractions gave the following yields: (A) 4.4, (B) 0.6, (C) 1.1 mg. The fractions were then analyzed by (i) NMR spectroscopy and (ii) derivatized and injected into a gas chromatography mass spectrometry (GC-MS) system.

NMR Spectroscopy. Solution-state NMR spectroscopy was carried out on a Bruker Avance 400 MHz instrument operating at a proton frequency of 400.13 MHz and a carbon frequency of 100.62 MHz. The spectrometer was equipped with a 5 mm Bruker inverse broadband probe with an actively shielded *z*-gradient coil. All of the spectra were acquired and elaborated by Bruker Topspin 1.3 software. Freeze-dried HPLC fractions were dissolved in 5 mm NMR quartz tubes using 0.55 mL of deuterated dimethyl sulfoxide (DMSO-d_6). ^{1}H NMR spectra were referenced to the chemical shift of the solvent, resonating at 2.51 ppm. Two-dimensional correlation spectroscopy (2D-COSY) experiments were acquired with a 16:12:40 gradient ratio (duration, 1 ms), 44 scans, 2000 points in F2, and 256 points in F1. COSY spectra were transformed with a sine−bell weighting function in both dimensions applying a sine−bell shift (SSB) of 0. Two dimensional total correlation spectroscopy (2D-TOCSY) spectra were acquired with a spin−lock period of 80 ms, 1000 points in F2, and 128 points in F1 with 32 scans. The spectra were transformed with a sine−bell weighting function in both dimensions with a SSB value of 0. Two-dimensional nuclear Overhauser effect spectroscopy (2D-NOESY) spectra were acquired by applying a mixing time of 0.8 s, 64 scans, 2000 points in F2, and 256 points in F1. Apodization was made by multiplying data with a squared sine function in both dimensions with a SSB value of 2. Two-dimensional ^{1}H−^{13}C heteronuclear single quantum coherence (HSQC) heterocorrelated experiments were acquired using a pulse field gradient sequence with a 80:20.1:11:−5 gradient ratio (duration, 1 ms), heteronuclear CH scalar coupling of 145 Hz, 2000 × 256 points in F2 and F1, respectively, and 100 scans. Data were multiplied by squared sine functions in both dimensions with a SSB value of 2. Two-dimensional diffusion-ordered spectroscopy (2D-DOSY) was performed using a bipolar gradient pulse sequence. Scans (160) were collected using 2.5 ms sine-shaped pulses (5 ms bipolar pulse pair) ranging from 0.674 to 32.030 G cm^{-1} in 32 increments with a diffusion time of 60 ms and 32 000 time domain data points. Apodization was made by multiplying data with an exponential function with a line broadening (LB) of

0.2 Hz. Diffusion coefficients of 10 standard compounds of known molecular weight were also measured to obtain a calibration curve of diffusion versus molecular weight from which molecular sizes of our reaction products were calculated (Figure 4). A solution of 1 mg in 0.55 mL of DMSO-d_6 was employed to obtain the DOSY spectra of the following standards: H_2O (18.0 Da), β-alanine (89.1 Da), catechol (110.1 Da), pyrogallol (126.1 Da), protocatechuic acid (154.1 Da), *p*-coumaric acid (164.2 Da), caffeic acid (180.2 Da), catechin (290.0 Da), quercetin (383.3 Da), and bromocresol green (698.0 Da).

Derivatization. Freeze-dried samples of isolated fractions were resolubilized in methanol and dried again under N_2 flux. The dried residues were redissolved in 50 μL of pyridine and silylated by adding 50 μL of *N*,*O*-bis(trimethylsilyl)-trifluoroacetamide/TMCS (99:1) and heating at 60 °C for 30 min.

Gas Chromatography−Mass Spectrometry. GC-MS analyses were conducted on a Perkin-Elmer Autosystem XL gas chromatograph, equipped with a Perkin-Elmer Turbomass Gold mass spectrometer. The derivatized samples (1 μL) were manually injected into the gas chromatograph equipped with (i) a capillary injector operated in splitless mode and maintained at a temperature of 250 °C and (ii) a Restek Rtx-5MS fused silica capillary column (30 m per 0.25 mm i.d., 0.25 μm film thickness). Helium was used as a carrier gas at a flow rate of 1.8 mL min^{-1}. The column oven was programmed with an initial temperature of 80 °C for 1 min, followed by a gradient from 80 to 180 °C at 4 °C/min, 180 to 320 °C at 10 °C/min, and a final temperature of 320 °C held for 10 min. The mass spectrometer was calibrated with tris(perfluoro-heptyl)-*s*-triazine and operated in the full scan mode, scanning in the range of *m*/*z* 50−1200 and using an electron impact ionization energy of 70 eV at a scan rate of 1.0 s/scan. Since the mass spectra of the expected oligomeric products are not provided by the National Institute of Standards and Technology library, identification of phenolic dimers was enabled by comparing their fragmentation patterns to that of the catechol monomer.[18]

Conformational Analysis by Computer Modeling. Geometry optimization was performed using a molecular dynamics simulation provided by Hyperchem, version 6.02. The initial structures of the catechol dimers were first only approximately optimized by applying 1000−1500 cycles of steepest descent minimization. The final conformational optimization was made by subjecting the previously roughly minimized dimers to the Polak−Ribiere conjugate gradient with a root-mean-square gradient of 0.01 kcal Å^{-1} mol^{-1}.

Results and Discussion

In the presence of H_2O_2, iron−porphyrin can undergo an oxidation giving highly reactive iron(IV) porphyrin cation radical species, which can catalyze the oxidation of phenol substrates into free radicals.[21,22] A free radical of dehydrogenated catechol may occur in four resonance forms (1−4 in Scheme 1) that may couple to each other to form dimers. Coupling reactions between the resonance forms (1 + 1), (1 + 2), (1 + 3), and (1 + 4) would result in C−O−C bonding and formation of oxyphenylene units, while C−C coupling and formation of phenylene units could be observed for the reaction between (2 + 2), (2 + 3), (2 + 4), (3 + 3), (3 + 4), and (4 + 4). A release of H_2O can be expected to accompany the coupling reactions involving the catechoyl radical 2 in Scheme 1 due to the loss of the hydroxyl attached to the aromatic carbon that hosts the unpaired electron.[23]

The fluorescence-detected HPLC chromatogram of the catechol oxidation products following the iron−porphyrin-catalyzed reaction is reported in Figure 1. Three major fractions were observed and isolated. Their elution times (A) 57.3, (B) 63.5, and (C) 68.0 min suggested that these products had lower polarities and higher molecular weights than the catechol monomer eluted at 44.0 min, while their intensive fluorescence indicated the presence of sufficiently conjugated systems.

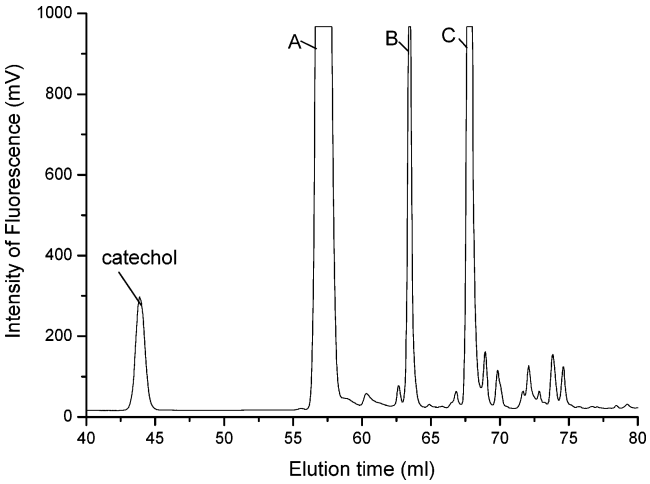

Figure 1. Fluorescence-detected chromatogram of products of catechol polymerization catalyzed by iron−porphyrin after 1 day of incubation. Peaks representing the reaction products are labeled A−C.

The GC-MS analysis of silylated fractions A, B, and C indicated in all cases the formation of a catechol dimer (*m*/*z* 506 Da) bonded through C−C coupling. However, the different retention times in the total ion chromatogram (31.5 min for fraction C, 32.2 min for B, and 33.8 min for A) suggested structural differences among the three fractions. The mass fragmentation patterns of A and B were similar but varied in intensities. This phenomenon is usually observed for different isomers of the same compound.[24] Therefore, a different position of the C−C bonding in the A and B dimers may be envisaged. The mass spectrum of fraction C was comparable to those of A, and B but showed an intensive ion at *m*/*z* 315 that could have resulted from a different fragmentation rearrangement caused by the conformational vicinity of the OH substituents on the ring. The mass spectra of A, B, and C are shown in Figure 2.

The C−C bonded dimers of catechol, corresponding to a *m*/*z* of 506 Da, could have resulted only from three possible combinations of coupling reactions between different resonance forms of the catechoyl radical (Scheme 1). These reactions would involve the coupling between the resonance forms (3 + 3), (3 + 4), and (4 + 4), as shown in Scheme 2. To distinguish the exact structure for each isolated C−C bonded dimer of catechol, the fractions isolated by HPLC separation were subjected to NMR analyses. Chemical shifts in ^{1}H and ^{13}C NMR spectra, including diffusion coefficients obtained from DOSY measurements, are shown in Table 1.

The ^{1}H NMR spectrum of A revealed only three aromatic protons, thereby suggesting a symmetric C−C dimer of catechol. The ABC system showed signals of a doublet at 6.88 ppm (^{1}H, J = 2.2 Hz), doublet of doublets at 6.77 ppm (^{1}H, J = 8.2 and 2.2 Hz), and another doublet at 6.73 ppm (^{1}H, J = 8.2 Hz). Since the coupling constant of 8 Hz reflects an ortho coupling, while a J = 2 Hz is characteristic for meta-positioned aromatic protons, compound A must have a proton in the ortho position and another one in the meta position, both relative to the 6.77 ppm proton. This interpretation is further supported by the

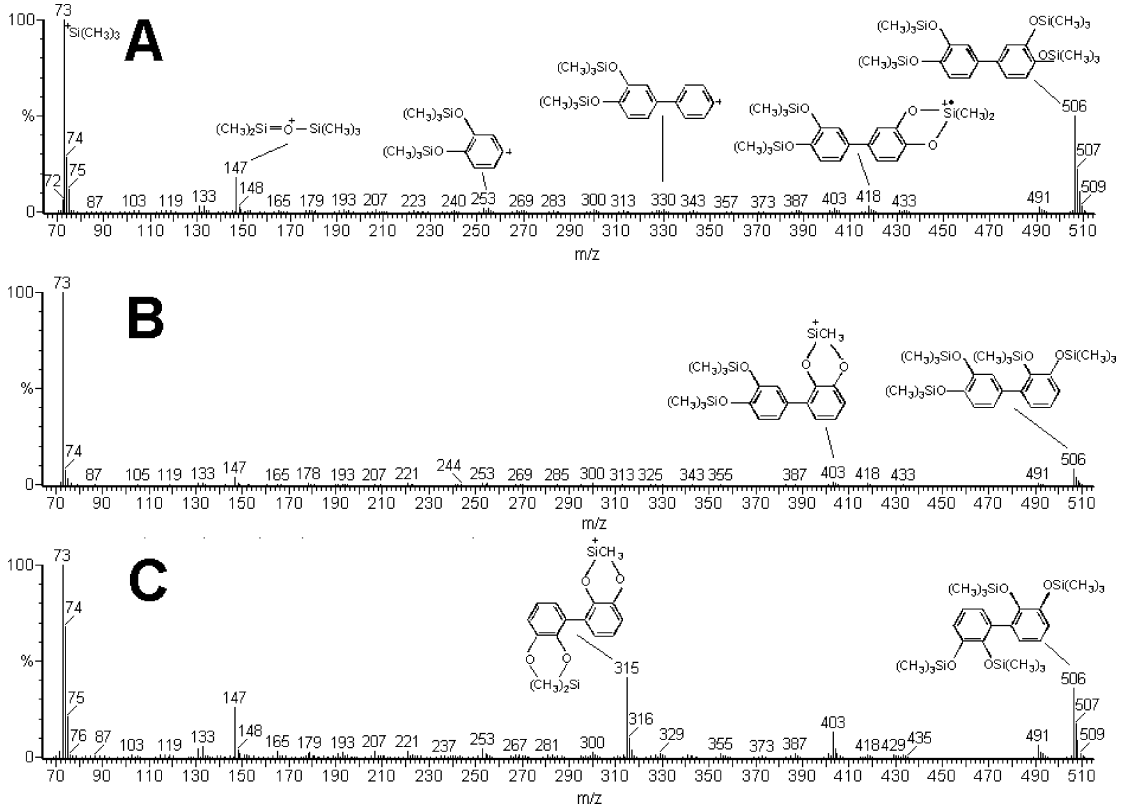

Figure 2. Mass spectra and suggested molecular fragmentation of tetrahydroxydiphenyl dimers A−C isolated as reaction products of catechol oxidative oligomerization induced by iron−porphyrin. Molecular fragments for similar *m*/*z* in A−C are shown only for one dimeric structure and are not repeated.

Table 1. ^{1}H and ^{13}C Chemical Shifts (δ) and Diffusion Coefficients (D) for DMSO Solutions of Fractionated Products A−C Formed during the Iron−Porphyrin-Catalyzed Oxidative Coupling of Catechol[a]

position in aromatic ring	δ (^{1}H, ppm)	multiplicity	J (Hz)	δ (^{13}C)[b]	$D \times 10^{-10}$ (m^2s^{-1})
		Dimer A			
2	6.88	d	2.2	114.0	2.00
5	6.73	d	8.2	116.6	2.02
6	6.77	dd	2.2/8.2	117.5	1.86
		Dimer B			
4	6.69	m		113.6	ND[c]
5	6.64	m		119.2[d]	ND
6	6.64	m		120.7[d]	ND
2′	6.97	d	2.0	116.9	ND
5′	6.72	d	8.2	115.3	ND
6′	6.77	dd	2.0/8.2	120.1	ND
		Dimer C			
4	6.79	d	8.0	112.4	2.08
5	7.05	dd	5.8, 8.0	123.5	2.26
6	7.29	d	5.7	110.5	2.28

[a] Chemical shifts of OH phenol groups were in all cases detected between 8 and 9 ppm and are not included in this table. [b] From 2D HSQC experiments. [c] Not determined. [d] Assignments may be interchanged.

presence of a cross-peak in the COSY contour plot (A in Figure 3), indicating correlation between protons at 6.77 and 6.88 ppm. The cross-peak corresponding to the correlation between the 6.73 and 6.77 ppm protons was not visible due to the overlay by the intensive diagonal peak centered at 6.75 ppm. DOSY analysis showed similar diffusion behavior for all detected signals of aromatic hydrogens and indicated that the molecular weight of compound A was in the region between 180 and 290 Da (Figure 4), thereby confirming the *m*/*z* value of the molecular ion detected by GC-MS. Furthermore, as expected for a symmetrically C−C bonded catechol dimer, the existence of three protonated aromatic carbons was confirmed in the ^{1}H−^{13}C HSQC correlation experiment (carbon chemical shifts are given in Table 1). The overall spectral assignments, combined with GC-MS results, unequivocally indicated that fraction A was the 3,4,3′,4′-tetrahydroxydiphenyl shown in Scheme 2 as dimer A.

The other possible symmetric C−C dimer of catechol, corresponding to the 2,3,2′,3′-tetrahydroxydiphenyl shown in Scheme 2, was assigned to fraction C. In fact, the ^{1}H NMR spectrum showed three sets of aromatic signals: a doublet at 6.79 ppm (^{1}H, J = 8.0 Hz), two doublets at 7.05 ppm (^{1}H, J = 5.8 and 8.0 Hz), and another doublet at 7.29 ppm (^{1}H, J = 5.7 Hz). Although the coupling constants of 5.8 and 5.7 Hz are not typical for ortho coupling in benzene ring systems, further analysis by COSY experiments attributed the 6.79 ppm signal to H4 (or its equivalent H4′), that at 7.05 ppm to H5 (or H5′), and that at 7.29 ppm to H6 (or H6′). The two cross-peaks showing connectivity between H6 and H5 and between H5 and H4 can be seen in Figure 3 (fraction C). The position of the diffusion signals in the DOSY spectrum corresponded to the molecular size region of a catechol dimer (Figure 4). Similarly, as in the previous case, the HSQC spectra gave evidence of only three protonated aromatic carbons (Table 1) and therefore supported the suggested structure of a catechol dimer deriving from the coupling between two similar catechoyl radicals, such as 4 in Scheme 1.

The ^{1}H NMR spectrum of B revealed the presence of six aromatic protons in the system and thus suggested the formation of a 2,3,3′,4′-tetrahydroxydiphenyl dimer. However, the assign-

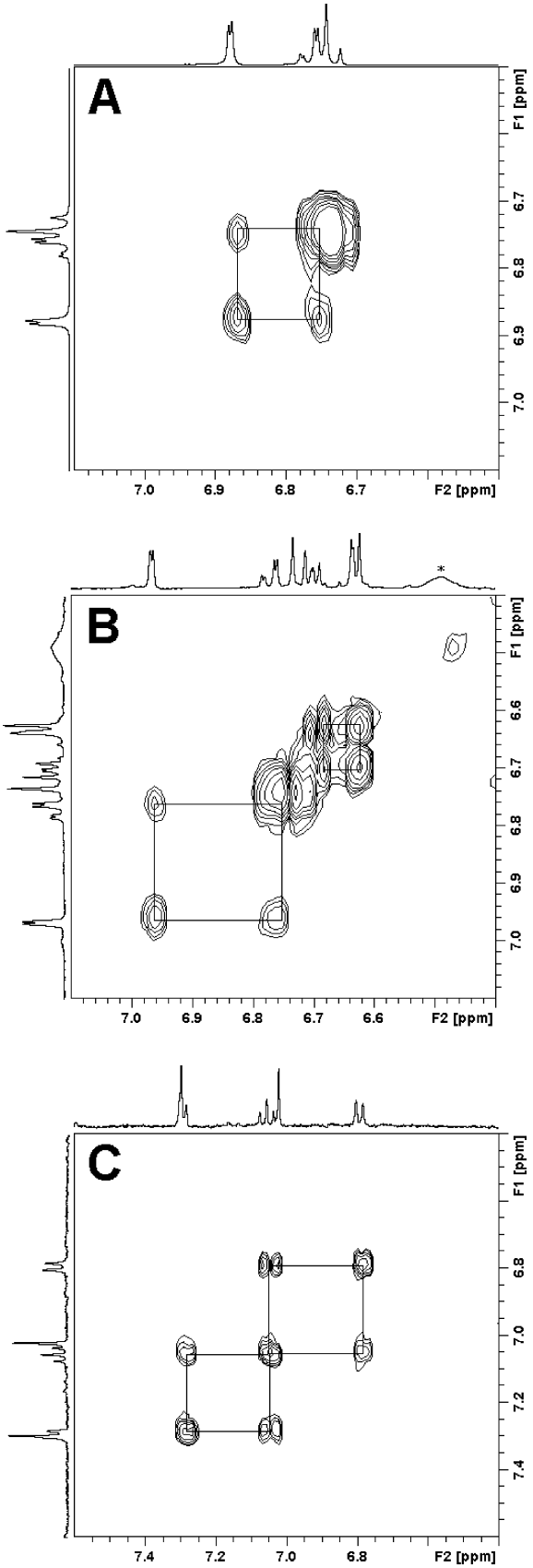

Figure 3. ^{1}H−^{1}H 2D-COSY NMR spectra of fractions A−C isolated as reaction products of catechol oxidative oligomerization catalyzed by iron−porphyrin. The signal labeled with a star does not show any correlation and is not related to the dimer.

ment of proton signals was not as straightforward as for the symmetric dimerizations. Doublets at 6.97 ppm (^{1}H, J = 2.0 Hz), 6.72 ppm (^{1}H, J = 8.2 Hz), and a doublet of doublets at 6.77 ppm (^{1}H, J = 8.2 and 2.0 Hz) generally reflected the splitting pattern of the 3′,4′-dihydroxyphenyl monomer of compound A, and the signals were initially attributed to H2′, H5′, and H6′ (Scheme 2, dimer B), respectively. The low-field shift of H2′ at 6.97 ppm (compared to H2 at 6.88 ppm in compound A) was taken as an indication of a possible presence of an anisotropic OH group in the close environment. However, the long-range anisotropic deshielding effect caused by the benzene ring of the second monomeric unit in the dimer cannot be excluded. Another interesting aspect in the magnetic behavior of this dimer was the absence of the expected well-resolved splitting pattern for H4, H5, and H6 (Scheme 2, dimer B) previously observed for the 2,3-dihydroxyphenyl monomer in fraction C. Conversely, a second-order splitting pattern into two multiplets was noted: a first one at 6.64 ppm (2H) and a second one at 6.69 ppm (1H). Both consisted of one singlet, one doublet, and a small side peak. A TOCSY experiment (spectrum not shown), performed only on fraction B, provided the necessary information about two different spin networks, one involving all proton signals in the range of 6.64−6.69 ppm and another one between 6.72 and 6.97 ppm. A COSY counter plot (Figure 3C) showed a correlation between H6′ and H2′ at 6.77 and 6.97 ppm, respectively, and another one between signals at 6.64 and 6.69 ppm. Unfortunately, a DOSY measurement did not reveal any diffusion coefficients for any of the aromatic protons. Therefore, in this case, a molecular weight supporting a catechol dimerization was indicated only by GC-MS analysis, which may not always reveal the true molecular ion. However, further structural evidence for an asymmetric catechol dimer was given by the HSQC spectra, which suggested the presence of six protonated aromatic carbons (Table 1).

To give an adequate explanation for the detection of the second-order splitting pattern obtained for H4, H5, and H6, and the low-field shift of H2′, the suggested structure of dimer B (Scheme 2) was geometrically optimized by the Hyperchem software, applying the Polak−Ribiere algorithm.[25] As shown in Figure 5, a spatially short distance of 2.8 Å was observed between H6 and H2′. This distance was comparable to 2.4−2.5 Å calculated for ortho-positioned protons in dimers A, B,

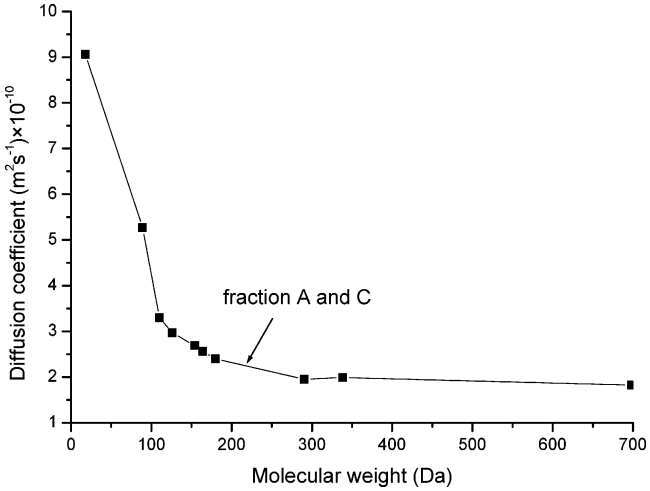

Figure 4. Diffusion coefficients of standard compounds and reaction products A and C as obtained from DOSY NMR spectra. Standard compounds from left to right are H_2O (18.0 Da), β-alanine (89.1 Da), catechol (110.1 Da), pyrogallol (126.1 Da), protocatechuic acid (154.1 Da), *p*-coumaric acid (164.2 Da), caffeic acid (180.2 Da), catechin (290.0 Da), quercetin (383.3 Da), and bromocresol green (698.0 Da).

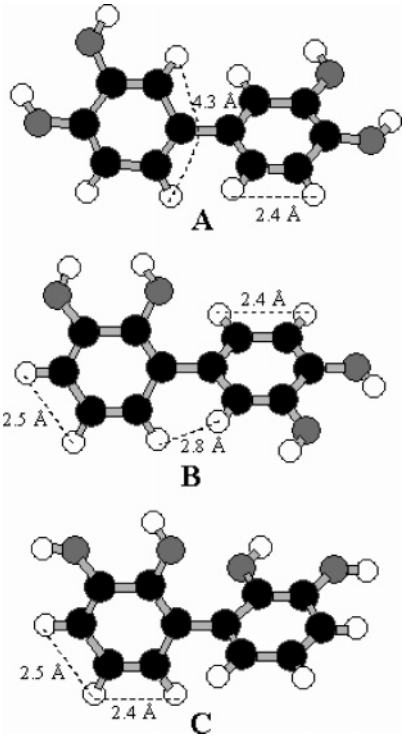

Figure 5. Optimized conformations of C−C bonded catechol dimers: (A) 3,4,3′,4′−tetrahydroxydiphenyl, (B) 2,3,3′,4′−tetrahydroxydiphenyl, and (C) 2,3,2′,3′−tetrahydroxydiphenyl. Black, gray, and white spheres represent carbon, oxygen, and hydrogen, respectively. Dotted lines show the calculated spatial distances between protons.

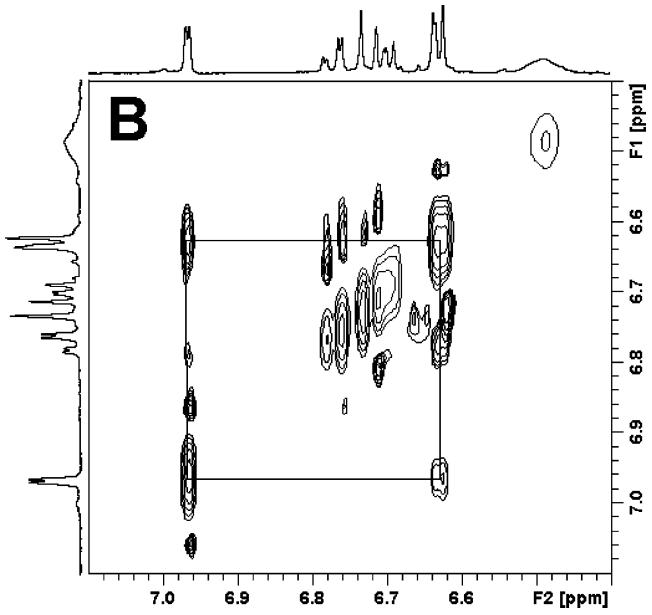

Figure 6. ^{1}H−^{1}H 2D-NOESY NMR spectrum of fraction B isolated as reaction products of catechol oxidative oligomerization catalyzed by iron−porphyrin.

and C and was even shorter than the distance of 4.3 Å observed for the meta-positioned protons in dimer A. The spatial vicinity of H6 and H2′ in dimer B may have led to dipolar interaction between these two hydrogens and consequently resulted in a through-space spin−spin coupling.

To confirm this suggestion, a NOESY experiment was performed on fraction B. Even though the NOESY diagram in Figure 6 contained some artifacts along the diagonal, a clear NOESY correlation was observed between H2′ resonating at 6.99 ppm and H6 at 6.64 ppm. Therefore, the low-field shift (6.99 ppm) at which H2′ resonates in the 3′,4′-dihydroxyphenyl monomer in fraction B (compared to 6.88 ppm in compound A) should not be attributed to the anisotropic effect of the OH phenol group in position 2 in the aromatic ring (Scheme 2, dimer B) but rather to the deshielding of this proton by the aromatic ring current of the 2,3-dihydroxyphenyl monomer. Although the spatial distance of 2.8 Å was also noted between H6 and H6′ in C, a similar possibility of spatial spin−spin coupling should be excluded, since these protons are chemically and magnetically equivalent. Considering the conformational models of dimers B and C, it is most likely that the occurrence of spatial spin−spin interactions in dimer B influenced the strength of spin−spin coupling among H4, H5, and H6 and resulted in the second-order splitting pattern. In fact, the existence of such strong coupling was also observed in the ^{1}H NMR spectrum of the catechol monomer (spectrum not shown).

On the basis of the NMR analyses, the mass spectra of A, B, and C shown in Figure 2 were attributed to the corresponding tetrahydroxydiphenyl isomers and consequently to their possible fragmentation ions. As previously suggested, the conformational vicinity of the OH substituents on the aromatic units in dimer C enabled the formation of a different fragmentation pathway of this dimer and yielded *m*/*z* at 315 (Figure 2), which was not detected for A and B.

Conclusions

This work has shown that the oxidative coupling of catechol catalyzed by a water-soluble iron−porphyrin leads to the formation of three major phenylene dimers. A number of NMR experiments on these dimers unequivocally elucidated their exact molecular structures as being: (A) 3,4,3′,4′-, (B) 2,3,3′,4′-, and (C) 2,3,2′,3′-tetrahydroxydiphenyl dimers. Since A and C were observed in larger amounts than B, the coupling reaction preferentially occurred between catechoyl radicals of the same resonance forms, in this case 3 and 4 in Scheme 1.

Acknowledgment. This work was partially supported by a grant from the Assessorato alla Ricerca Scientifica della Regione Campania. D.S. gratefully acknowledges the fellowship received within this grant to conduct research in Portici. The NMR work was conducted at the Centro Interdipartimentale di Risonanza Magnetica Nucleare at the Facoltà di Agraria (Portici) of the Università di Napoli Federico II.

References and Notes

(1) Adrian, P.; Andreux, F.; Metche, M.; Mansour, M.; Korte, F. *C.R. Acad. Sci., Ser. II* **1986**, *303*, 1615−1618.
(2) Stevenson, F. J. *Humus Chemistry: Genesis, Composition, and Reactions*, 2nd ed.; Wiley: New York, 1994.
(3) Sánchez-Cortés, S.; Francioso, O.; García−Ramos, J. V.; Ciavatta, C.; Gessa, C. *Colloids Surf., A* **2001**, *176*, 177−184.
(4) Dec, J.; Haider, K.; Bollag, J.-M. *Soil Sci.* **2001**, *166*, 660−671.
(5) Dec, J.; Haider, K.; Bollag, J.-M. *Chemosphere* **2003**, *52*, 549−556.
(6) Martin, J. P.; Haider, K. *Soil Sci.* **1971**, *3*, 54−63.
(7) Majchner, E. H.; Chorover, J.; Bollag, J.-M.; Huang, P. M. *Soil Sci. Soc. Am. J.* **2000**, *64*, 157−163.
(8) Borraccino, R. M.; Kharoune, M.; Giot, R.; Agathos, S.; Nyns, E.-J.; Naveau, H. P.; Pauss, A. *Water Res.* **2001**, *35*, 3729−3737.
(9) Ward, G.; Parales, R. E.; Dosoretz, C. G. *Environ. Sci. Technol.* **2004**, *38*, 4753−4757.
(10) Zeichmann, W. *Z. Pflanzenernaehr. Dueng. Bodenkd.* **1959**, *84*, 155−159.
(11) Wang, T. S. C.; Wang, M. C.; Huang, P. M. *Soil Sci.* **1983**, *136*, 226−230.
(12) Aktaş, N.; Tanyolaç, A. *J. Mol. Catal. B: Enzym.* **2003**, *22*, 61−69.
(13) Ahn, M.-Y.; Martínez, C. E.; Archibald, D. D.; Zimmerman, A. R.; Bollag, J.-M.; Dec, J. *Soi Biol. Biochem.* **2006**, *38*, 1015−1020.

(14) Dubey, S.; Singh, D.; Misra, R. A. *Enzyme Microb. Technol.* **1998**, *23*, 432−437.
(15) Naidja, A.; Huang, P. M.; Bollag, J.-M. *Soil Sci. Soc. Am. J.* **1998**, *62*, 188−195.
(16) Aktaş, N.; Tanyolaç, A. *Bioresour. Technol.* **2003**, *87*, 209−214.
(17) Dordick, J.; Marletta, M. A.; Klibanov, A. M. *Biotechnol. Bioeng.* **1987**, *30*, 31−36.
(18) Šmejkalová, D.; Piccolo, A.; Spiteller, M. *Environ. Sci. Technol.* **2006**, *40*, 6955−6962.
(19) Piccolo, A.; Conte, P.; Tagliatesta, P. *Biomacromolecules* **2005**, *6*, 351−358.
(20) Šmejkalová, D.; Piccolo, A. *Environ. Sci. Technol.* **2006**, *40*, 1644−1649.
(21) Groves, J. T.; Haushalter, R. C.; Nakamura, M.; Nemo, T. E.; Evans, B. J. *J. Am. Chem. Soc.* **1981**, *103*, 2884−2886.
(22) Sheldon, R. A. In *Metalloporphyrins in Catalytic Oxidations*; Sheldon, R. A., Ed.; Marcel Dekker: New York, 1994; pp 12−15.
(23) Dec, J.; Bollag, J.-M. *Environ. Sci. Technol.* **1994**, *28*, 484−490.
(24) Ichimura, K.; Yasuhiro, A.; Akiyama, H.; Kudo, K.; Hayashi, Y. *Macromolecules* **1997**, *30*, 903−911.
(25) Khoda, K. M.; Liu, Y.; Storey, C. *J. Optim. Theory Appl.* **1992**, *75*, 345−354.

BM060598O